

# Galaxy Occupation Statistics of Dark Matter Haloes: Observational Results

Xiaohu Yang<sup>1</sup>, H.J. Mo<sup>1</sup>, Y.P. Jing<sup>2</sup>, Frank C. van den Bosch<sup>3</sup>  $\star$

<sup>1</sup>*Department of Astronomy, University of Massachusetts, Amherst MA 01003-9305, USA*

<sup>2</sup>*Shanghai Astronomical Observatory; the Partner Group of MPA, Nandan Road 80, Shanghai 200030, China*

<sup>3</sup>*Department of Physics, Swiss Federal Institute of Technology, ETH Hönggerberg, CH-8093, Zurich, Switzerland*

## ABSTRACT

We study the occupation statistics of galaxies in dark matter haloes using galaxy groups identified from the 2-degree Field Galaxy Redshift Survey with the halo-based group finder of Yang et al. (2004b). The occupation distribution is considered separately for early and late type galaxies, as well as in terms of central and satellite galaxies. The mean luminosity of the central galaxies scales with halo mass approximately as  $L_c \propto M^{2/3}$  for haloes with masses  $M < 10^{13} h^{-1} M_\odot$ , and as  $L_c \propto M^{1/4}$  for more massive haloes. The characteristic mass of  $10^{13} h^{-1} M_\odot$  is consistent with the mass scale where galaxy formation models suggest a transition from efficient to inefficient cooling. Another characteristic halo mass scale,  $M \sim 10^{11} h^{-1} M_\odot$ , which cannot be probed directly by our groups, is inferred from the conditional luminosity function (CLF) that matches the observed galaxy luminosity function and clustering. For a halo of given mass, the distribution of  $L_c$  is rather narrow. Detailed comparison with mock galaxy redshift surveys indicates this implies a fairly deterministic relation between  $L_c$  and halo mass. The satellite galaxies, however, are found to follow a Poissonian number distribution, in excellent agreement with the occupation statistics of dark matter subhaloes. This provides strong support for the standard lore that satellite galaxies reside in subhaloes. The central galaxies in low-mass haloes are mostly late type galaxies, while those in massive haloes are almost all early types. We also measure the CLF of galaxies in haloes of given mass. Over the mass range that can be reliably probed with the present data ( $13.3 \lesssim \log[M/(h^{-1} M_\odot)] \lesssim 14.7$ ), the CLF is reasonably well fit by a Schechter function. Contrary to recent claims based on semi-analytical models of galaxy formation, the presence of central galaxies does not show up as a strong peak at the bright end of the CLF. The CLFs obtained from the observational data are in good agreement with the CLF model obtained by matching the observed luminosity function and large-scale clustering properties of galaxies in the standard  $\Lambda$ CDM model.

**Key words:** dark matter - large-scale structure of the universe - galaxies: haloes - methods: statistical

## 1 INTRODUCTION

According to the current paradigm of structure formation, galaxies form and reside inside extended cold dark matter (CDM) haloes. These haloes are virialized clumps that formed through the gravitational instability of the cosmic density field, and have typical sizes that are much smaller than their mean spatial separation. One of the ultimate challenges in astrophysics is to obtain a detailed understanding of how galaxies with different physical properties occupy dark matter haloes of different mass. This link between

galaxies and dark matter haloes is an imprint of various complicated physical processes related to galaxy formation, such as gravitational instability, gas cooling, star formation, merging, tidal stripping and heating, and a variety of feedback processes. A detailed quantification of this link is therefore pivotal for our understanding of galaxy formation and evolution within the CDM cosmogony. Although the statistical link itself does not give a physical explanation of how galaxies form and evolve, it provides important constraints on these processes and on how their efficiencies scale with halo mass.

To quantify the relationship between haloes and galaxies in a statistical way, it has become customary to specify

$\star$  E-mail: xhyang@astro.umass.edu

the so-called halo occupation distribution,  $P(N|M)$ , which gives the probability to find  $N$  galaxies (with some specified properties) in a halo of mass  $M$ . This occupation distribution can be constrained using data on the clustering properties of galaxies, as it completely specifies the galaxy bias, and has been used extensively to study the galaxy distribution in dark matter haloes and the galaxy clustering on large scales (Jing, Mo & Börner 1998; Peacock & Smith 2000; Seljak 2000; Scoccimarro et al. 2001; Jing, Börner & Suto 2002; Berlind & Weinberg 2002; Bullock, Wechsler & Somerville 2002; Scranton 2002; Kang et al. 2002; Marinoni & Hudson 2002; Zheng et al. 2002; Magliocchetti & Porciani 2003; Berlind et al. 2003; Zehavi et al. 2004a,b; Zheng et al. 2004).

Since individual galaxies are not featureless objects, but have diverse intrinsic properties, a more useful halo occupation model should contain some information regarding the physical properties of the galaxies. A significant step in this direction has been taken by Yang, Mo & van den Bosch (2003b) and van den Bosch, Yang & Mo (2003a), who modelled the halo occupation as a function of both galaxy luminosity and type (see also Vale & Ostriker 2004 for a somewhat different approach). In particular, they introduced the conditional luminosity function (CLF),  $\Phi(L|M)dL$ , which gives the average number of galaxies with luminosity  $L \pm dL/2$  that reside in a halo of mass  $M$ . As shown by Yang et al. (2003b), once the galaxy luminosity function and the galaxy correlation amplitude as a function of luminosity are known, tight constraints on  $\Phi(L|M)$  can be obtained. Detailed comparisons with additional data from the 2dFGRS, the Sloan Digital Sky Survey (SDSS) and DEEP2 have shown that the resulting halo occupation models can reproduce a large number of observations regarding the galaxy distribution at low redshift (Yan, Madgwick & White 2003; Yang et al. 2004a; Mo et al. 2004; Wang et al. 2004; Zehavi et al. 2004b; Yan, White & Coil 2004). This not only implies that these occupation distributions provide a reliable description of the connection between galaxies and CDM haloes, it also implies that the standard  $\Lambda$ CDM model is a good approximation to the real Universe. After all, the abundances and clustering properties of dark matter haloes are cosmology dependent, and matching the data with occupation models is only possible for a restricted set of cosmological parameters (Zheng et al. 2002; van den Bosch et al. 2003b; Rozo, Dodelson & Frieman 2004; Abazajian et al. 2004).

An important shortcoming of these occupation models, however, is that the results are not completely model independent. Typically assumptions have to be made regarding the functional form of either  $P(N|M)$  or  $\Phi(L|M)$ . For example, in our work on the CLF we have always assumed that it is well described by a Schechter function (Yang et al. 2003b; van den Bosch et al. 2003a, 2004b). Recently, however, the validity of this assumption was questioned by Zheng et al. (2004), based on a study of the conditional baryonic mass function (similar to the CLF but with luminosity replaced by baryonic mass) in semi-analytical models of galaxy formation. Note that in all halo occupation studies to date, the occupation distributions have been determined in an indirect way: the free parameters of the assumed functional form are constrained using *statistical* data on the abundance and clustering properties of the galaxy popula-

tion. Ideally, however, one would determine the occupation distribution more directly, by using a method that can determine which galaxies belong to the same dark matter halo. If such a method can be found, the occupation statistics, including the CLF, can be obtained directly from the data without the need to make any assumptions.

In this paper we perform such a direct determination of the occupation statistics using the halo-based group finder developed by Yang et al. (2004b). Detailed tests with mock galaxy catalogues have shown that this group finder is very successful in associating galaxies according to their common dark matter haloes (Yang et al. 2004b,c). In particular, the group finder performs reliably not only for rich systems, but also for poor systems, including isolated central galaxies in low-mass haloes, making it possible to study the galaxy-halo connection for a wide range of different systems. In this paper, we use the sample of galaxy groups obtained from the 2dFGRS with this group finder to study the galaxy occupation statistics in dark matter haloes as a function of halo mass, galaxy luminosity and type, and in terms of both central and satellite galaxies. The arrangement of the paper is as follows: In Section 2 we describe the data and the mock surveys used in the present paper. Sections 3 and 4 presents our results on the halo occupation distribution and on the CLF. Further discussion and a summary of our results are given in Section 5.

## 2 GROUP CATALOGUES

### 2.1 Galaxy Groups in the 2dFGRS

Here we briefly describe the group catalogues used in the analyzes that follow. The construction of these catalogues, as well as numerous tests regarding the performance of the group finder, is described in Yang et al. (2004b, hereafter YMBJ) to which we refer the interested reader for details.

The basic idea behind the group finder developed by YMBJ is similar to that of the matched filter algorithm developed by Postman et al. (1996) (see also Kepner et al. 1999; White & Kochanek 2002; Kim et al. 2002; Kochanek et al. 2003; van den Bosch et al. 2004a,b), although it also makes use of the galaxy kinematics. The group finder starts with an assumed mass-to-light ratio to assign a tentative mass to each potential group (identified using the Friends-of-Friends (FOF) method). This mass is used to estimate the size and velocity dispersion of the underlying halo that hosts the group, which in turn is used to determine group membership (in redshift space). This procedure is iterated until no further changes occur in group memberships. The performance of the group finder was tested in terms of completeness of true members and contamination by interlopers, using detailed mock galaxy redshift surveys. The average completeness of individual groups is  $\sim 90$  percent and with only  $\sim 20$  percent interlopers. Furthermore, the resulting group catalogue is insensitive to the initial assumption regarding the mass-to-light ratios, and the group finder is more successful than the conventional FOF method (e.g., Eke et al. 2004 and references therein) in associating galaxies according to their common dark matter haloes.

In YMBJ we used this group finder to identify galaxy groups in the final public data release of the 2dFGRS. This

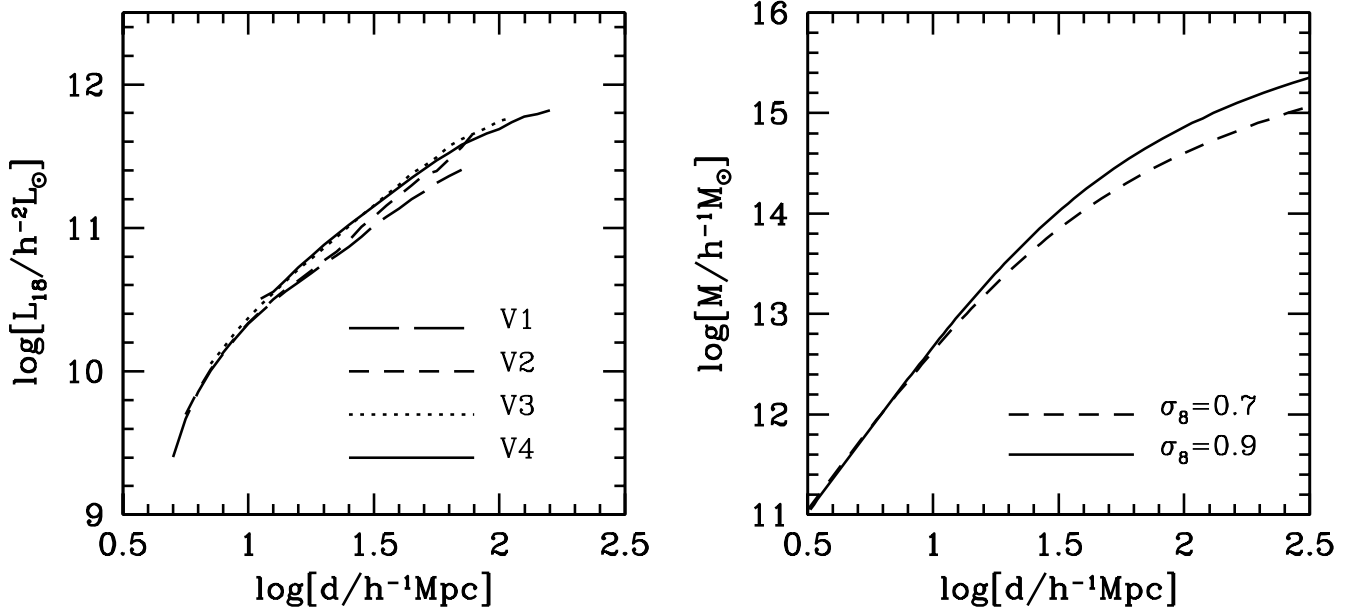


**Figure 1.** The left-hand panel shows the relation between the group luminosity  $L_{18}$  and the mean separation  $d$  of all groups with a group luminosity larger than  $L_{18}$ . Different lines correspond to different ‘mass-limited’ group samples obtained from the 2dFGRS (see Table 1). The small differences at large  $d$  are due to cosmic variance. The right-hand panel shows the relation between the halo mass  $M$  and mean halo separation  $d$  derived from the mass function of dark matter haloes for two  $\Lambda$ CDM cosmologies with different  $\sigma_8$ , as indicated. Throughout this paper we compute halo masses from group luminosities as follows: for a group with given  $L_{18}$  we determine the mean separation  $d$  between all groups with a group luminosity larger than  $L_{18}$ , and use the panel on the right to determine the halo mass  $M$  that corresponds to this  $d$  for the cosmology under consideration.

redshift sample of galaxies contains about 250,000 galaxies and is complete to an extinction-corrected apparent magnitude of  $b_J \approx 19.45$  (Colless et al. 2001). When identifying galaxy groups, we restricted ourselves to galaxies with redshifts  $0.01 \leq z \leq 0.20$  in the North Galactic Pole (NGP) and the South Galactic Pole (SGP) regions. Only galaxies with redshift quality parameter  $q \geq 3$  and with redshift completeness  $> 0.8$  were used. This left a grand total of 151,280 galaxies with a sky coverage of  $1124 \text{ deg}^2$ . From this sample, YMBJ obtained a group catalogue that contains 78,708 systems, of which 7251 are binaries, 2343 are triplets, and 2502 are systems with four or more members. In what follows we use this group catalogue to determine the halo occupation statistics of the 2dFGRS.

## 2.2 Mock Group Catalogues

In testing the halo-based group finder, YMBJ used a set of detailed mock galaxy redshift surveys (hereafter MGRSs). Here we use these same MGRSs for comparison with the 2dFGRS. For the present analysis, we correct these MGRSs for close pair incompleteness that arises from fiber collisions and from the fact that nearby galaxies overlap (so that they are identified as a single galaxy, rather than a galaxy pair). The method used to correct our MGRSs for both these effects is described in detail in van den Bosch et al. (2004b). Note that this close-pair incompleteness has only a minor impact on our results: in other words, if we were not to correct for these effects, it would not impact any of our main conclusions. In what follows, we give a brief description about how these MGRSs are constructed, and we refer

the reader to Yang et al. (2004a) and van den Bosch et al. (2004a) for details.

The mock surveys are constructed by populating dark matter haloes in large numerical simulations with galaxies of different luminosities and different types. The simulations correspond to a  $\Lambda$ CDM concordance cosmology with  $\Omega_m = 0.3$ ,  $\Omega_\Lambda = 0.7$ ,  $h = H_0/(100 \text{ km s}^{-1} \text{ Mpc}^{-1}) = 0.7$  and with a scale-invariant initial power spectrum with normalization  $\sigma_8 = 0.9$ , and all MGRSs discussed in this paper are therefore only valid for this particular cosmology. To populate the dark matter haloes with galaxies we use the CLF. Because of the mass resolution of the simulations and because of the completeness limit of the 2dFGRS we adopt a minimum galaxy luminosity of  $L_{\min} = 10^7 h^{-2} L_{\odot}$  throughout. The *mean* number of galaxies with  $L \geq L_{\min}$  that resides in a halo of mass  $M$  is given by

$$\langle N \rangle_M = \int_{L_{\min}}^{\infty} \Phi(L|M) dL \quad (1)$$

In order to Monte-Carlo sample occupation numbers for individual haloes one requires the full probability distribution  $P(N|M)$  (with  $N$  an integer) of which  $\langle N \rangle_M$  gives the mean, i.e.,

$$\langle N \rangle_M = \sum_{N=0}^{\infty} N P(N|M) \quad (2)$$

We use the results of Kravtsov et al. (2004a), who has shown that the number of *subhaloes* follows a Poisson distribution. In what follows we differentiate between satellite galaxies, which we associate with these dark matter subhaloes, and central galaxies, which we associate with the

host halo. The total number of galaxies per halo is the sum of  $N_{\text{cen}}$ , the number of central galaxies which is either one or zero, and  $N_{\text{sat}}$ , the (unlimited) number of satellite galaxies. We assume that  $N_{\text{sat}}$  follows a Poisson distribution and require that  $N_{\text{sat}} = 0$  whenever  $N_{\text{cen}} = 0$ . The halo occupation distribution is thus specified as follows: if  $\langle N \rangle_M \leq 1$  then  $N_{\text{sat}} = 0$  and  $N_{\text{cen}}$  is either zero (with probability  $P = 1 - \langle N \rangle_M$ ) or one (with probability  $P = \langle N \rangle_M$ ). If  $\langle N \rangle_M > 1$  then  $N_{\text{cen}} = 1$  and  $N_{\text{sat}}$  follows the Poisson distribution

$$P(N_{\text{sat}}|M) = e^{-\mu} \frac{\mu^{N_{\text{sat}}}}{N_{\text{sat}}!}, \quad (3)$$

with  $\mu = \langle N_{\text{sat}} \rangle_M = \langle N \rangle_M - 1$ .

We follow Yang et al. (2004a) and van den Bosch et al. (2004b) and assume that the central galaxy is the brightest galaxy in each halo. Its luminosity is drawn from  $\Phi(L|M)$  with the restriction that  $L > L_1$  with  $L_1$  defined by

$$\int_{L_1}^{\infty} \Phi(L|M) dL = 1. \quad (4)$$

The luminosities of the satellite galaxies are also drawn at random from  $\Phi(L|M)$ , but with the restriction  $L_{\text{min}} < L < L_1$ .

Note that the resulting occupation statistics are not fully Poissonian. To investigate whether such a deviation from Poissonian can be detected from the statistics of galaxy groups we also, for comparison, construct a MGRS in which the *full*  $P(N|M)$  is Poissonian (not only that of the satellites), and in which all  $N$  galaxies are drawn from the CLF without any restriction other than  $L \geq L_{\text{min}}$ . In what follows we refer to the MGRSs based on the  $L_1$ -restricted luminosity sampling as our ‘fiducial’ mocks, and to those with the unrestricted, Poissonian sampling as the ‘Poisson’ mocks.

The positions and velocities of the galaxies with respect to the halo center-of-mass are drawn assuming that the central galaxy in each halo resides at rest at the center. The satellite galaxies follow a number density distribution that is identical to that of the dark matter particles, and are assumed to be in isotropic equilibrium within the dark matter potential. To construct MGRSs we use the same selection criteria and observational biases as in the 2dFGRS, making detailed use of the survey masks provided by the 2dFGRS team (Colless et al. 2001; Norberg et al. 2002). Using a set of independent numerical simulations, we construct 8 independent MGRSs which we use to address scatter due to cosmic variance. The MGRSs thus constructed accurately match the clustering properties, the apparent magnitude distribution and the redshift distribution of the 2dFGRS, allowing for a direct comparison. Finally, for each MGRS we construct group samples using the same halo-based group finder and the same group selection criteria as for the 2dFGRS.

Our fiducial MGRS, used throughout this paper, is based on the best-fit CLF listed in Table 1 (the model with ID  $\Lambda_{0.9}$ ) of van den Bosch et al. (2004b). This CLF predicts an average mass-to-light ratio on the scale of clusters of  $(M/L)_{\text{cl}} = 500h$  ( $M/L$ ) $_{\odot}$ . Although in fair agreement with independent observational constraints (e.g., Carlberg et al. 1996; Bahcall et al. 2000, but see also Tully 2003), we have shown that both the pairwise peculiar velocity dispersions and the group multiplicity function of the 2dFGRS suggest a significantly higher cluster mass-to-light ratio of

**Table 1.** ‘Mass-limited’ group samples from the 2dFGRS

| Sample | $z_{\text{max}}$ | $\log L_{18,\text{min}}$<br>$h^{-2} L_{\odot}$ | $N_{\text{grp}}$ | $\log d$<br>$h^{-1} \text{Mpc}$ | $\log M_{\text{min}}$<br>$h^{-1} M_{\odot}$ |
|--------|------------------|--|------------------|---------------------------------|---|
| (1)    | (2)              | (3)  | (4)              | (5)                             | (6)   |
| V1     | 0.08             | 9.4  | 11682            | 0.70                            | 11.7  |
| V2     | 0.09             | 9.6  | 13578            | 0.73                            | 11.8  |
| V3     | 0.14             | 10.0   | 24069            | 0.83                            | 12.1  |
| V4     | 0.20             | 10.5   | 13510            | 1.07                            | 12.9  |

Column (1) indicates the sample ID. The selection criteria used to define these samples are indicated in Columns (2) and (3), which list the maximum redshift  $z_{\text{max}}$  (sample galaxies obey  $0.01 < z < z_{\text{max}}$ ) and the minimum group luminosity  $L_{18,\text{min}}$ , respectively. Columns (4) and (5) list the number of groups in each sample,  $N_{\text{grp}}$ , and the mean group separation,  $d$ , respectively. Finally, column (6) lists the corresponding minimum halo mass,  $M_{\text{min}}$ , obtained using the relation between  $d$  and  $M$  shown in the left-hand panel of Fig. 1 (assuming  $\sigma_8 = 0.9$ ).

$(M/L)_{\text{cl}} = 900h$  ( $M/L$ ) $_{\odot}$  (Yang et al. 2004a,b). We therefore also construct a set of MGRSs based on the CLF with  $(M/L)_{\text{cl}} = 900h$  ( $M/L$ ) $_{\odot}$  (see Yang et al. 2004b), using the same sampling strategy as with our fiducial mocks. Although the model with  $(M/L)_{\text{cl}} = 500h$  ( $M/L$ ) $_{\odot}$  is preferred by the observed galaxy-galaxy clustering strength, the data is not sufficient to rule out a cluster mass-to-light ratio as high as  $900h$  ( $M/L$ ) $_{\odot}$  (see van den Bosch et al. 2004b).

### 2.3 Ranking halo mass according to group luminosity

In order to infer halo occupation statistics from our group samples it is crucial that we can estimate the halo masses associated with the groups. For individual, rich clusters one could in principle estimate halo masses using the kinematics of the member galaxies, gravitational lensing of background sources, or the temperature profile of the X-ray emitting gas. For most groups, however, no X-ray emission has been detected, and no lensing data is available. In addition, the vast majority of the groups in our sample contain only a few members, making a dynamical mass estimate based on its members extremely unreliable. We thus need to adopt a different approach to estimate halo masses.

As discussed in YMBJ, for each group one can define a characteristic luminosity,  $L_{18}$ , defined as the total luminosity of all group members brighter than  $M_{b_J} - 5 \log h = -18$ . For groups at relatively high redshift  $L_{18}$  can not be measured directly because of the apparent magnitude limit of the survey. For these groups we estimate  $L_{18}$  from the luminosity of the observable group members, using a correction factor that is calibrated using relatively nearby groups (see Yang et al. (2004b,c) for details). Tests with MGRSs have shown that  $L_{18}$  is tightly correlated with the mass of the dark matter halo hosting the group. As shown in Yang et al. (2004c), ranking groups according to  $L_{18}$  is therefore similar to mass-ranking, allowing the construction of reliable, ‘mass-limited’ group samples. In Table 1, we list the ‘mass-limited’ group samples used in this paper. Each sample is specified by two selection criteria; a lower limit on  $L_{18}$ , which as we argued above translates into a lower limit on halo mass, and a maximum redshift  $z_{\text{max}}$ . The latter assures

that each sample is complete to some absolute magnitude limit, which is required for a meaningful comparison of the group member galaxies.

In order to convert the  $L_{18}$ -ranking to the corresponding halo mass,  $M$ , we use the mean group separation,  $d = n^{-1/3}$ , as a mass indicator. Here  $n$  is the number density of all groups brighter (in terms of  $L_{18}$ ) than the group in consideration. In the left panel of Fig. 1, we plot the mean relation between the group luminosity  $L_{18}$  and the mean group separation  $d$  for 2dF groups, with different lines corresponding to different ‘mass-limited’ subsamples. Overall the  $L_{18}$ - $d$  relation is similar for different subsamples. The small, but noticeable, differences reflect cosmic variance due to the presence of a few very large structures in the 2dFGRS (see e.g., Baugh et al. 2004). Since  $L_{18}$  is tightly correlated with halo mass, we can convert  $d$  to  $M$ . Unfortunately, this conversion requires knowledge of the halo mass function, and thus knowledge of the cosmological parameters. As discussed in Section 2.2, throughout this paper we consider a  $\Lambda$ CDM concordance cosmology with  $\sigma_8 = 0.9$ . To illustrate how sensitive the  $d$ -to- $M$  conversion depends on the rather uncertain power-spectrum normalization parameter, the right-hand panel of Fig. 1 plots the  $M$ - $d$  relations for both  $\sigma_8 = 0.9$  and  $\sigma_8 = 0.7$ . For haloes with masses  $M \lesssim 10^{13.5} h^{-1} M_\odot$ , the  $M$ - $d$  relation is virtually independent of  $\sigma_8$ . For  $M \gtrsim 10^{13.5} h^{-1} M_\odot$ , however,  $d$  is smaller in the  $\sigma_8 = 0.9$  cosmology simply because massive haloes are more abundant in cosmologies with larger  $\sigma_8$ . Unless specifically stated otherwise, we use the  $\sigma_8 = 0.9$  model to convert  $d$  to  $M$ , but we emphasize that any function of  $M$  can be converted back into a function of  $d$  using the relation represented by the solid curve in the right-hand panel of Fig. 1.

### 3 HALO OCCUPATION STATISTICS FROM 2DFGRS GROUPS

Having assigned 2dFGRS galaxies into groups according to their common dark matter haloes, we now present a detailed investigation of the halo occupation statistics, describing how galaxies with different physical properties are associated with dark matter haloes of different mass.

#### 3.1 The halo occupation distribution

The upper three panels of Fig. 2 plot the occupation numbers of galaxies in 2dFGRS groups as a function of  $d$  (which, as discussed above, can be used as a proxy for halo mass). Results are shown for galaxies with  $M_{b,j} - 5 \log h < -18.0$  (left panel),  $-19.0$  (middle panel) and  $-20.0$  (right panel), respectively. These occupation numbers are obtained using the summation  $N = \sum 1/c_i$ , with  $c_i$  the completeness in the 2dFGRS at the position of galaxy  $i$ , so that  $N$  is not necessarily an integer. The lower three panels of Fig. 2 plot the same occupation numbers but this time obtained from our fiducial MGRS, using exactly the same method as for the 2dFGRS. Note that in the construction of the MGRS we use completeness maps of the 2dFGRS. Therefore, we can compute exactly the same  $N$  for our mock groups (i.e., summation of  $c_i$ ) as in the real 2dFGRS. Although the occupation statistics of the groups in the MGRS reveal overall

the same behavior as those in the 2dFGRS, there are some noticeable differences, which we quantify in more detail below.

The upper panels of Fig. 3 plot the *mean* halo occupation numbers,  $\langle N \rangle$ , as a function of  $d$  for the same samples of 2dFGRS groups as in Fig. 2. Using the  $M$ - $d$  relations shown in Fig. 1 we convert these into the average occupation numbers as function of halo mass shown in the bottom panels. Note that the average occupation numbers increase with halo mass, as expected. At the low mass end, however, they reveal a relatively flat shoulder and a sharp break, both at  $\langle N \rangle \sim 1$ . This sharp break seems to indicate an almost deterministic relation between the luminosity of the central (brightest) galaxy in each halo and the mass of the halo, while the shoulder suggests that the second brightest galaxy is significantly fainter than the brightest one (e.g., Zheng et al. 2004). The dotted curves with errorbars indicate the occupation numbers obtained from the groups in our fiducial MGRS. These reveal an almost identical shoulder plus break. The dashed lines, however, indicate the  $\langle N \rangle_M$  obtained directly from the CLF used to construct the MGRS (computed from eq. [1] with  $L_{\min}$  the minimum luminosity of the sample under consideration). The agreement of these *true* occupation statistics with those inferred from the MGRS group catalogues is remarkably good at  $\langle N \rangle \gtrsim 1$ , indicating that the conversion of  $L_{18}$  to halo mass via the mean separation  $d$  does not introduce any systematic error. It also shows that the groups identified with the method developed in Yang et al. (2004b) can be used to accurately probe halo occupation statistics. For  $\langle N \rangle \lesssim 1$ , however, there is a noticeable discrepancy between the true  $\langle N \rangle_M$  and that obtained from the MGRS. In particular, the shoulder and sharp break at  $\langle N \rangle \simeq 1$  visible in the mean occupation numbers of the mock groups are not present in the true  $\langle N \rangle_M$ . The origin of this discrepancy is easy to understand if one takes the stochasticity of the occupation numbers into account. Since we estimate halo masses from the  $L_{18}$ -ranking, halo masses are overestimated if they happen to contain a relatively bright galaxy (compared to the mean). Similarly, haloes with a relatively faint galaxy compared to the mean will have their masses underestimated. If the average luminosity is close to the luminosity limit of the sample, this stochasticity in the occupation statistics causes a systematic deviation from the true  $\langle N \rangle_M$ , as the haloes with the relatively faint galaxies will not make the sample selection criteria. Caution is therefore required in interpreting the sharp break and the shoulder around  $N = 1$  seen in the occupation statistics of the 2dFGRS groups. Although they may still be real, we cannot rule out that they are simply artifacts due to combined effect of stochasticity and magnitude limit.

The lower panels of Fig. 3 also show that our fiducial MGRSs predict too many galaxies per group at the high mass end. Given the errorbars, which reflect the scatter among 8 fiducial MGRSs, these differences are very significant. As we discuss in Section 3.2, this reflects a problem with the number of satellite galaxies, and suggests either a high mass-to-light ratio on the scale of galaxy clusters, or a reduction of the power-spectrum normalization  $\sigma_8$  from the fiducial value of 0.9 to  $\sim 0.7$ . This is easy to understand: increasing the mass-to-light ratio on the scale of clusters, basically implies fewer galaxies per cluster. Since the to-

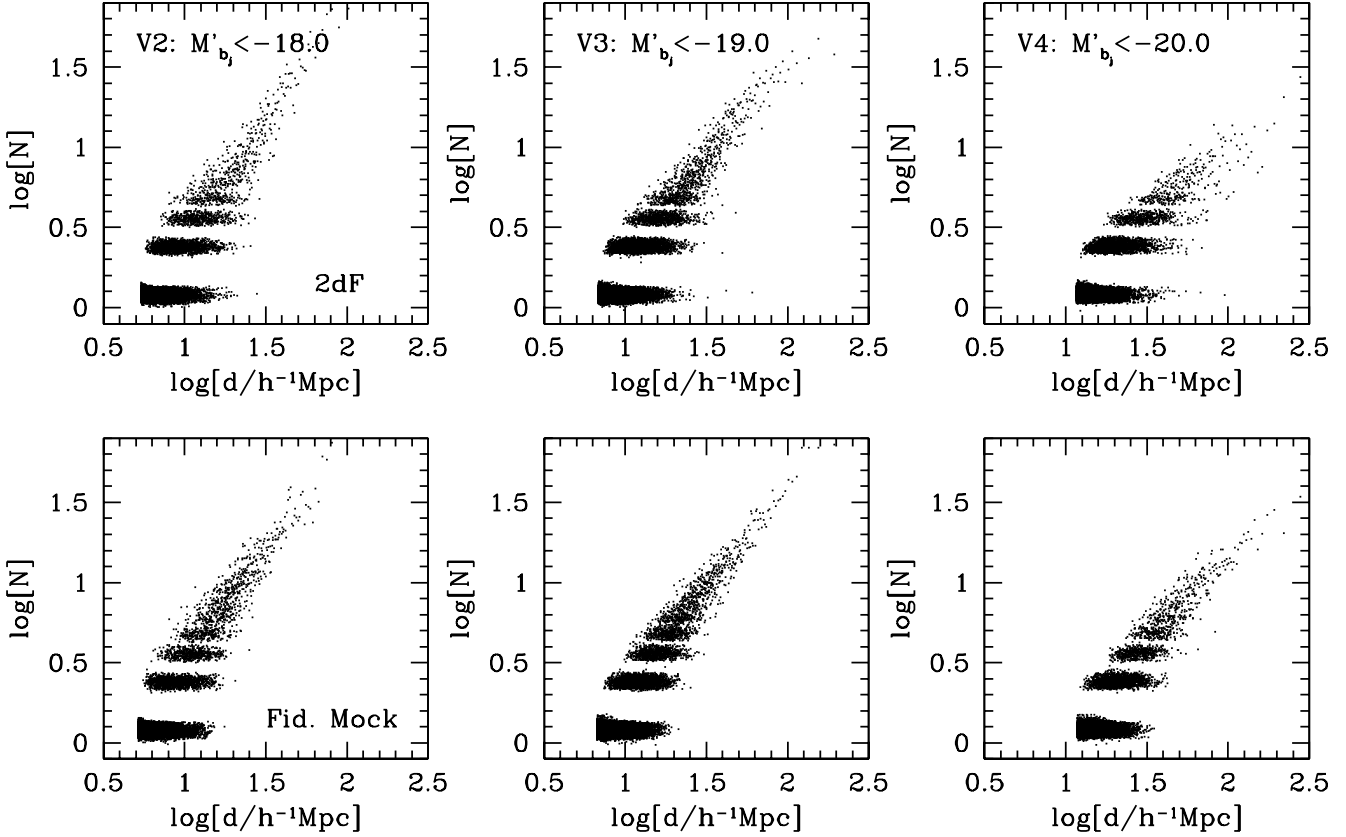


**Figure 2.** The halo occupation number distributions for groups in the 2dFGRS (upper panels) and one realization of the fiducial MGRS (lower panels) as a function of the group mean separation  $d$ . The left-, middle and right-hand panels correspond to different ‘mass-limited’ samples with an absolute magnitude limit of  $M'_{b_J} = M_{b_J} - 5 \log h$ . Note that the occupation numbers are corrected for incompleteness effects, which explains their non-integer nature.

tal number density of galaxies is conserved (constrained by the galaxy luminosity function), these galaxies now need to be distributed over lower mass haloes. Therefore, increasing  $(M/L)_{\text{cl}}$  decreases  $\langle N \rangle$  for the most massive haloes, while (mildly) increasing  $\langle N \rangle$  for the less massive haloes. Note that, since less massive haloes are less strongly clustered, an increase of  $(M/L)_{\text{cl}}$  lowers the overall clustering strength of the galaxy population. However, as shown in van den Bosch, Mo & Yang (2003b) and van den Bosch et al. (2004a), there is a sufficient amount of freedom in the data to allow us to modify  $(M/L)_{\text{cl}}$  and still get a reasonable match to the data. It is this freedom that we exploit here to argue for a high value of  $(M/L)_{\text{cl}}$ . An alternative solution to the mismatch between the  $\langle N \rangle_M$  of MGRS and 2dFGRS is to lower  $\sigma_8$ . Lowering  $\sigma_8$  reduces the number of massive haloes, but changes little the clustering strength of haloes at a given mass (the decrease in the clustering strength of dark matter particles is largely compensated by the increase in the bias factor). If the value of  $(M/L)_{\text{cl}}$  is fixed, lowering  $\sigma_8$  requires more galaxies to be assigned to lower-mass haloes, and the net effect on galaxy clustering is similar to that with a higher value of  $(M/L)_{\text{cl}}$  (Yang et al. 2004a; van den Bosch et al. 2004b).

In addition to the *mean* occupation numbers, we also investigate the second moment of the halo occupation distribution. This quantity is required in the modelling of the two-point correlation function of galaxies on small scales (e.g.,

Benson et al. 2000; Berlind et al. 2003; Yang et al. 2004a), and holds important information regarding the physical processes related to galaxy formation. In earlier investigations, a number of simple models were adopted to describe the second moment of the halo occupation distribution and its dependence on halo mass (e.g., Berlind & Weinberg 2002). With our group samples, we can actually measure this quantity directly. We present our results in terms of the ratio between the standard deviation,  $\sigma(N)$ , and the square root of the mean,  $\sqrt{\langle N \rangle}$ . Since for a Poisson distribution  $\sigma(N)/\sqrt{\langle N \rangle} = 1$ , this ratio expresses the amount of stochasticity relative to Poisson. The solid lines in Fig. 4 show the results obtained from the 2dFGRS, where the three panels correspond to the same volume-limited samples as in Figs. 2 and 3. The ratio  $\sigma(N)/\sqrt{\langle N \rangle}$  is close to unity in massive haloes, but reveals a pronounced minimum at low  $M$ . This suggests that the halo occupation distribution is (close to) Poissonian in massive haloes and significantly sub-Poissonian in low mass haloes.

Note, however, that because of our method of assigning masses, Fig. 4 really shows the scatter in  $N$  at given  $L_{18}$ . In order to test how the scatter in the relation between  $M$  and  $L_{18}$  impacts on these results, we compare our findings with those obtained from a MGRS that is identical to our fiducial MGRS, except that this time the central galaxy is not treated in any special way, so that the occupation distri-

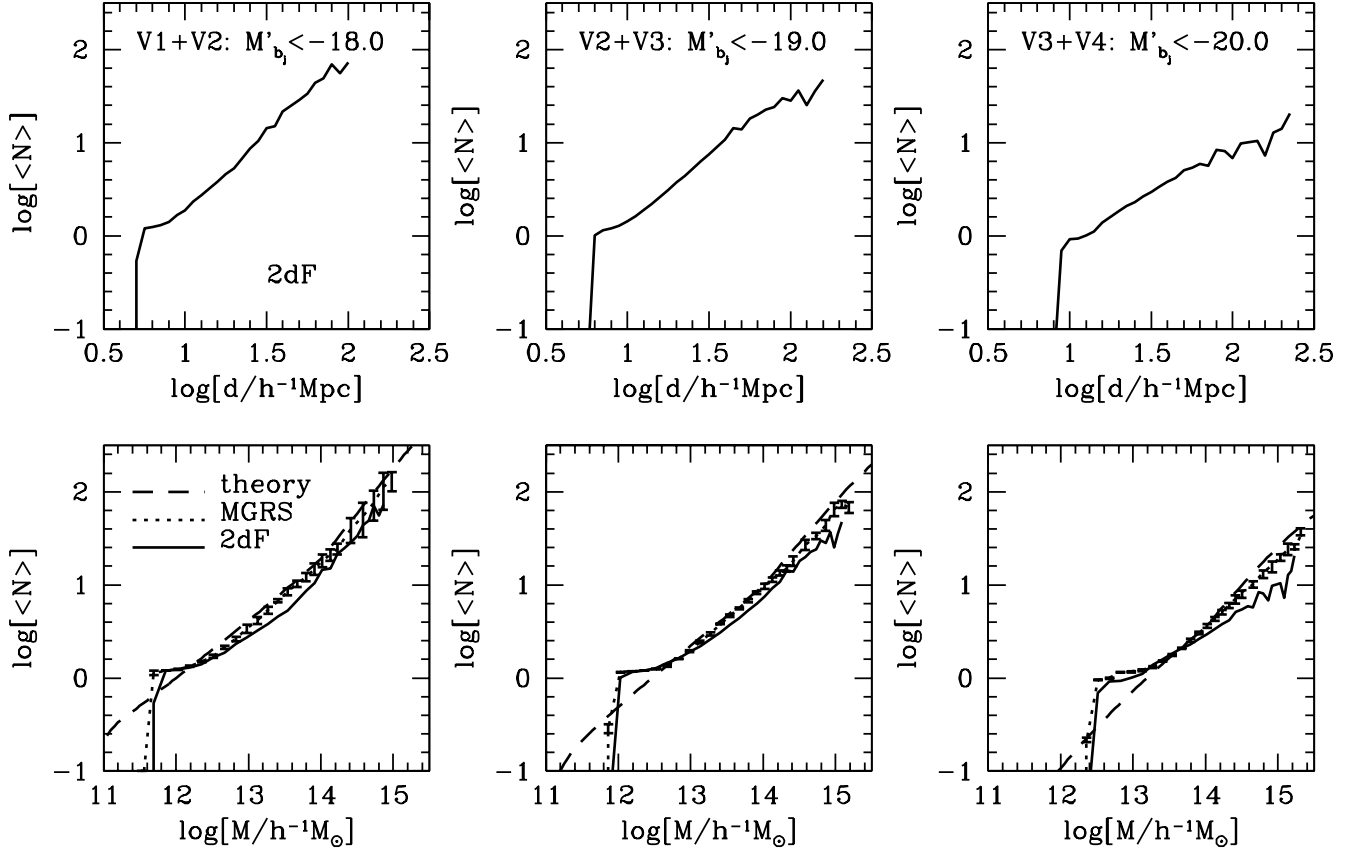


**Figure 3.** The mean halo occupation numbers as a function of mean group separation  $d$  (upper panels) and halo mass (lower panels). Solid lines correspond to groups in the 2dFGRS. The dotted lines with errorbars in the lower panels show the results obtained from the groups in our fiducial MGRSs. The errorbars are obtained from the  $1\text{-}\sigma$  scatter among 8 independent MGRSs. The dashed lines in the lower panels, labelled ‘theory’, indicate the true, mean occupation numbers, obtained directly from the CLF (eq. [1]) used to construct the MGRS. A comparison with the dotted lines shows that the halo occupation numbers are well recovered, except for groups with  $\langle N \rangle < 1$ , where an artificial shoulder and break are introduced. The comparison between 2dFGRS and MGRS shows that our fiducial model predicts too many galaxies per group at the high mass end (see text for a detailed discussion).

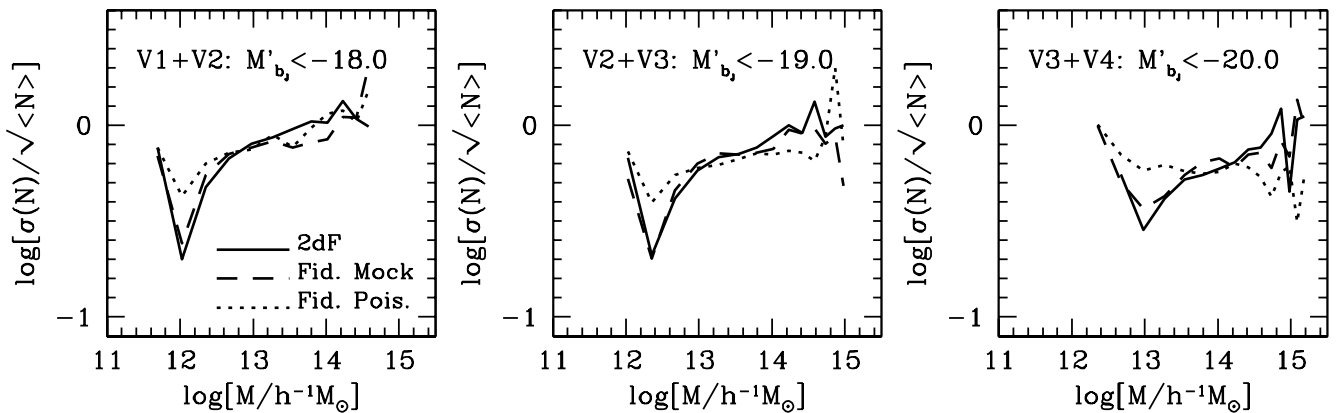


**Figure 4.** The scatter of the halo occupation number distribution, expressed in terms of the ratio between the standard deviation,  $\sigma(N)$ , and the square root of the mean,  $\sqrt{\langle N \rangle}$ . Note that this ratio is equal to unity for a Poisson distribution. Results are shown as function of halo mass  $M$  for the same ‘mass-limited’ groups samples as in Figs 2 and 3. The solid and dashed lines correspond to the results obtained from the groups in the 2dFGRS and the fiducial MGRS, respectively, and are in excellent agreement with each other. The dotted lines correspond to a MGRS that is similar to the fiducial one, except that the luminosity of the central galaxy is not treated in a special way (i.e., the true occupation statistics are purely Poissonian in this case). Since halo masses are estimated from the ranking of  $L_{18}$ , the ratio deviates from unity even for this pure Poisson case. See the text for a detailed discussion regarding the interpretation of these results.

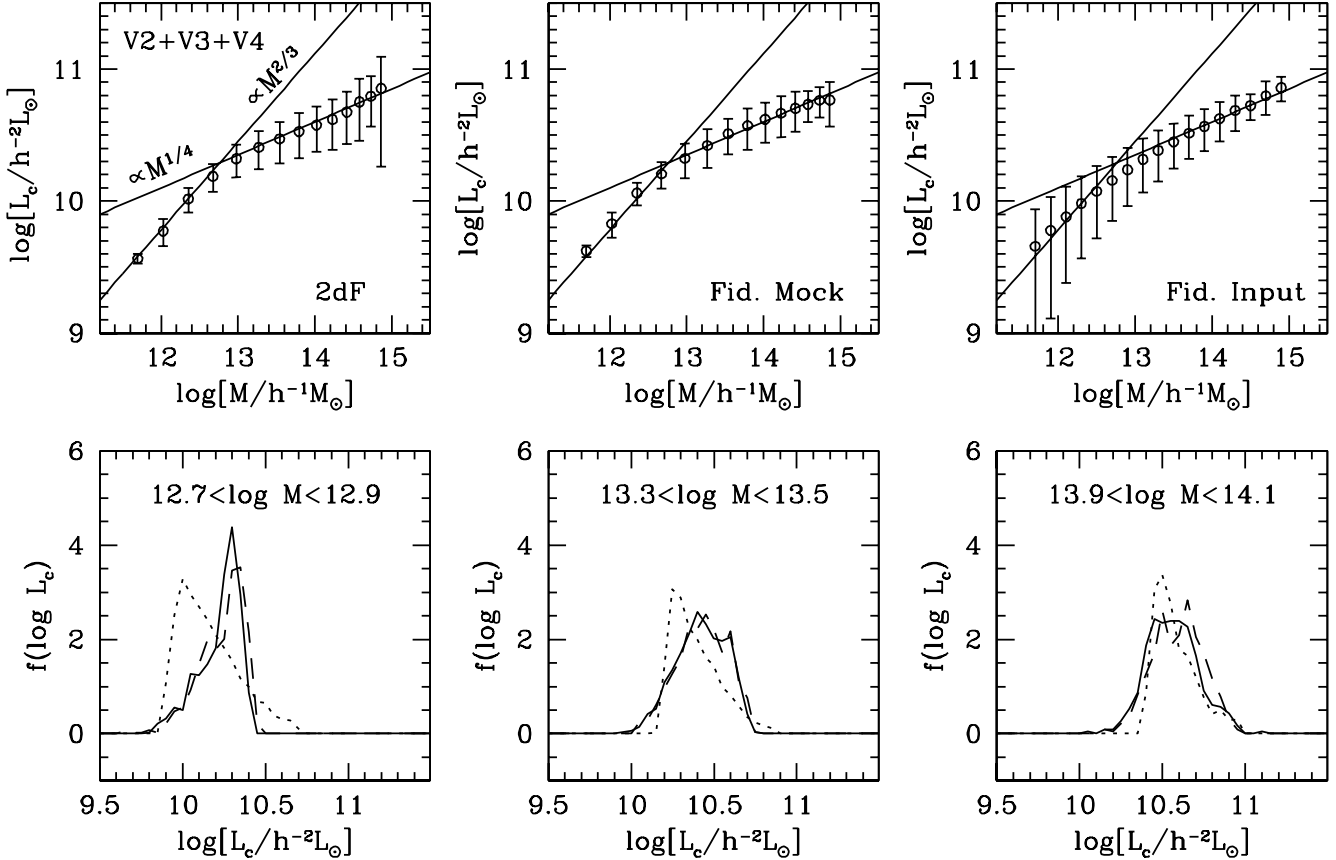


**Figure 5.** The upper panels plot the mean central galaxy luminosity,  $L_c$ , as function of halo mass,  $M$ , with the errorbars indicating the  $1\text{-}\sigma$  scatter around the mean. The left and middle panel correspond to the 2dFGRS and the fiducial MGRS, respectively, where we have used the ‘mass-limited’ samples V2, V3, and V4 (see Table 1). Solid lines indicate two power-law relations, and are indicated to facilitate a comparison. Note the excellent agreement between the 2dFGRS and the MGRS. The upper right-hand panel indicates the same relation between  $L_c$  and  $M$ , but this time determined directly from the populated haloes in our simulation box (i.e., without making a mock redshift surveys from which we select groups). Although the mean  $L_c - M$  relation is virtually identical to that derived from the mock groups, the scatter is significantly larger in low mass haloes (see text for discussion). The lower panels plot the distributions  $P(L_c|M)$  for three different bins in halo mass, as indicated. Solid, dashed, and dotted curves correspond to the 2dFGRS, the fiducial MGRS, and the simulation box, respectively.

bution,  $P(N|M)$ , is completely Poissonian (see Section 2.2). Any deviation of  $\sigma(N)/\sqrt{\langle N \rangle}$  from unity in this MGRS is therefore completely artificial, allowing us to assess the robustness of our findings. The dotted curves in Fig. 4 show the results obtained from this MGRS. They reveal a small minimum in  $\sigma(N)/\sqrt{\langle N \rangle}$  at small  $M$ , similar though less pronounced than for the 2dFGRS. The origin of this artefact is similar to that of the artificial shoulder and break in the *mean* occupation numbers. In haloes with  $\langle N \rangle \simeq 1$  one expects a significant fraction of haloes with  $N = 0$ ; in fact, for a Poissonian  $P(N|M)$  the probability to have  $N = 0$  is almost 40 percent. These haloes, however, do not appear in the group samples causing an overestimate of  $\langle N \rangle$  and an underestimate of the variance. Therefore, the ratio  $\sigma(N)/\sqrt{\langle N \rangle}$  is underestimated for haloes with  $\langle N \rangle \simeq 1$ . The upturn at the very low-mass end is due to the (artificial) sharp break in  $\langle N \rangle$ , which drives  $\sigma(N)/\sqrt{\langle N \rangle}$  up again. The presence of these artefacts clearly demonstrates the importance of using detailed MGRSs to properly interpret the data.

The dashed lines in Fig. 4 show the results obtained from our *fiducial* MGRS. These results are in excellent agree-

ment with those obtained from the 2dFGRS, indicating that the CLF and the method used for its sampling agree well with the data. As indicated in Section 2.2, the occupation statistics of the central galaxies are treated differently than those of the satellite galaxies: whereas  $P(N|M)$  is Poissonian for the latter, central galaxies follow a much narrower nearest-integral distribution. This means that  $P(N|M)$  is strongly sub-Poissonian whenever  $\langle N \rangle$  is small. As is evident from a comparison with Fig. 3, the minimum in  $\sigma(N)/\sqrt{\langle N \rangle}$  occurs at a halo mass where the average occupation number is virtually unity. This, together with the fact that the minimum in  $\sigma(N)/\sqrt{\langle N \rangle}$  is much more pronounced than in the pure-Poissonian MGRS, leads us to conclude that (i) the number of satellite galaxies above a certain luminosity limit follow a Poissonian distribution, and (ii) the occupation statistics of central galaxies are sub-Poissonian, indicating some deterministic behavior in galaxy formation. Clearly, a detailed study of the higher-order moments of the occupation statistics can yield important constraints on galaxy formation, and we intend to return to this in more detail in a forthcoming paper.



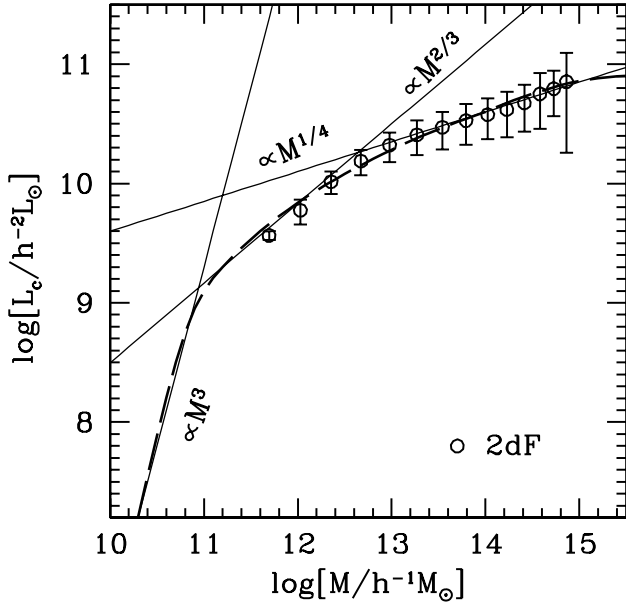


**Figure 6.** The mean central galaxy luminosity,  $L_c$ , as function of halo mass,  $M$ , over a large range in haloes masses. The data points are the same as those shown in the upper left panel of Fig 5. The dashed curve is the  $L_c$ - $M$  relation given by the CLF obtained from matching the observed luminosity function of galaxies and the correlation length as a function of galaxy luminosity. Note the existence of another characteristic mass scale,  $M \simeq 10^{11} h^{-1} M_\odot$ , below which  $L_c$  decreases rapidly with decreasing  $M$ . This plot indicates that scaling relations such as the Tully-Fisher relation hold only over a limited range of halo masses.

### 3.2 Central versus satellite galaxies

In theoretical models of galaxy formation, galaxies in dark matter haloes are usually separated into central galaxies and satellite galaxies. Since central and satellite galaxies are expected to have somewhat different formation histories (e.g., Kauffmann, White & Guiderdoni 1993), it is interesting to study the halo occupation distribution separately for these two categories of galaxies. By definition, the central galaxy in a halo should be the one that is located near the center of the host halo. Since in theory the central galaxy is expected to be the most massive one among all galaxies in the halo, we have defined the brightest galaxy in a group (halo) as the central galaxy, and the others as satellite galaxies.

The upper panels of Fig. 5 plot the relation between the luminosity of the central galaxy,  $L_c$ , and the mass of the host halo,  $M$ . Results are shown both for groups in the 2dFGRS (left panel) and for those in our fiducial MGRS (middle panel). We also show the true relation between  $L_c$  and  $M$  (right panel) obtained directly from the populated haloes in our simulation box (i.e., without making a mock redshift surveys from which we select groups). The mean  $L_c$ - $M$  relation is remarkably similar for all three samples, and well described by a broken power-law with  $L_c \propto M^{2/3}$  at  $M \lesssim 10^{13} h^{-1} M_\odot$  and  $L_c \propto M^{1/4}$  at  $M \gtrsim 10^{13} h^{-1} M_\odot$ . At the low-mass end, this is in excellent agreement with results based on galaxy-galaxy weak lensing, which imply that  $M \propto L_c^{1.5}$  (e.g. Yang et al. 2003a; Guzik & Seljak 2002). At the massive end,  $L_c$  only increases very slowly with halo mass, which is consistent with the recent result

obtained by Lin et al. (2004), indicating that there must be a physical process that prevents the central galaxies in massive haloes from growing. One possibility is that radiative cooling of halo gas becomes negligible in massive haloes, with  $M \simeq 10^{13} h^{-1} M_\odot$  the characteristic mass that marks the transition from effective to ineffective cooling (cf., Dekel 2004). The requirement for such a transition is well known from semi-analytical models of galaxy formation where it is required to reproduce the bright end of the observed luminosity function (e.g., White & Rees 1978; Kauffmann et al. 1993; Benson et al. 2003; Kang et al. 2004).

The errorbars in the upper panels of Fig. 5 indicate the scatter around  $L_c$  at given  $M$ . Except for some small discrepancies at high  $M$ , the amounts of scatter in the 2dFGRS and MGRS are very similar. This is illustrated more clearly in the lower panels of Fig. 5, which plot the actual distributions of  $L_c$  for three bins in halo mass (as indicated) for both the 2dFGRS (solid lines) and the MGRS (dashed lines). Overall the agreement is remarkably good, providing strong support for the CLF and its sampling strategy. Note that the  $P(L_c|M)$  look similar to log-normal distributions, with a fairly narrow width that depends only mildly on halo mass.

To properly interpret these findings we compare these  $P(L_c|M)$  with those obtained directly from the populated haloes in the simulation box (i.e., without making a mock redshift surveys from which we select groups). As evident from the upper-right panel of Fig. 5, at low  $M$  the scatter in the *true*  $L_c - M$  relation is much larger than in the relation inferred from the mock group catalogue. This is also evident from the lower panels in Fig. 5 which show that the true  $P(L_c|M)$  (dotted curves) in haloes with  $M \lesssim 10^{13} h^{-1} M_\odot$  is significantly broader than the inferred distribution. In particular, the inferred distribution seems to lack predominantly the low- $L_c$  galaxies. This discrepancy arises from the stochasticity in the  $L_{18} - M$  relation. In low-mass haloes, where the average occupation number is close to unity,  $L_{18}$  is basically identical to  $L_c$ . This means that the  $L_{18}$ -ranking becomes similar to  $L_c$ -ranking, so that the resulting  $L_c - M$  relation becomes virtually scatter free. In addition, because of the magnitude limit of the group sample, the haloes with relatively faint central galaxies are missed, causing a deficit of low- $L_c$  galaxies. On the other hand, some central galaxies may be missed in the sample because of observational selection effects, and so some of the galaxies identified as the central galaxies are actually the second or even the third brightest galaxy in a group. This introduces extra scatter in  $L_c$ , which causes the scatter at the high-mass end to be larger for the MGRSs (and the 2dFGRS) than the *true* scatter. Therefore, as with the scatter in the occupation numbers, great care is required when interpreting the scatter in  $P(L_c|M)$ . In particular, the log-normal character of  $P(L_c|M)$  of the 2dFGRS galaxies does not necessarily imply that the true distribution is log-normal. We emphasize, however, that despite this bias, the comparison between the 2dFGRS and the MGRS is still meaningful. In particular, the good agreement between both group catalogues suggests that our method of assigning galaxies to dark matter haloes used in the construction of the MGRS (see Section 2.2) is in excellent agreement with the 2dFGRS.

Since our group sample becomes quite incomplete for halos with  $M \lesssim 10^{12} h^{-1} M_\odot$ , we cannot use our groups to

study the  $L_c$ - $M$  relation for low-mass haloes. However, our CLF, which is constrained by the abundances and clustering properties of the galaxy population, *does* contain such information. The dashed curve in Fig. 6 shows the  $L_c$ - $M$  relation obtained from our CLF down to haloes with  $M = 10^{10} h^{-1} M_\odot$ . For comparison, we also plot the results obtained from our 2dFGRS group catalogue, which are in excellent agreement with these predictions. For haloes with  $M \lesssim 10^{12} h^{-1} M_\odot$ , however, no reliable determination of  $L_c(M)$  can be obtained from the groups. This is unfortunate as our CLF model predicts the presence of a second characteristic mass scale at  $M \simeq 10^{11} h^{-1} M_\odot$ . For haloes below this scale  $L_c$  is predicted to decrease rapidly with decreasing  $M$  (roughly as  $L_c \propto M^\beta$ , with  $\beta \sim 2 - 4$ ). This is required in order to match the relatively steep slope of the halo mass function at the low mass end with the relatively shallow faint-end slope of the galaxy luminosity function (see e.g., Yang et al. 2003b), and is often interpreted as ‘evidence’ for a suppression of star formation by feedback effects (e.g. Dekel & Silk 1986; Dekel 2004). Note that the  $L_c$ - $M$  relation shown in Fig. 6 suggests that scaling relations such as the Tully-Fisher relation can hold only over a limited range of halo masses.

Let us now move on to satellite galaxies. Fig. 7 plots the distribution of the number of satellite galaxies in groups,  $N_s$ , for a number of different mass bins. The thick solid curves indicate Poisson distributions with the same  $\langle N_s \rangle$ , and fit the  $N_s$ -distributions extremely well. This is an important result, because it suggests a direct link between satellite galaxies and dark matter subhaloes. In a recent study, Kravtsov et al. (2004), using large numerical simulations, have shown that the occupation distribution of dark matter subhaloes follows a Poisson distribution, in excellent agreement with the occupation statistics of the satellite galaxies shown here.

For comparison, the dotted lines in Fig. 7 plot the distributions of  $N_s$  obtained from our fiducial MGRS. Unlike with the central galaxies, for which MGRS and 2dFGRS are in excellent agreement, the MGRS contains far too many satellite galaxies in massive systems. This explains the discrepancy in the average occupation numbers  $\langle N \rangle$  at large  $M$  shown in Fig. 3, and is consistent with the findings in some of our previous studies (Yang et al. 2004a; YMBJ; van den Bosch et al. 2004b). As discussed in Yang et al. (2004a), there are two different ways to reduce the number of rich systems. One is to increase the mass-to-light ratio of clusters, so that the number of galaxies assigned to a massive halo is reduced. The other is to reduce the value of  $\sigma_8$ , so that the number of massive haloes that can host a large number of satellite galaxies is reduced. As an illustration, the dashed lines in Fig. 7 show the results obtained from a MGRS based on the CLF model with  $(M/L)_{\text{cl}} = 900 h (M/L)_\odot$  (see Section 2.2). This model matches the 2dFGRS distributions much better. Similar results are obtained if we reduce the value of  $\sigma_8$  to  $\sim 0.70$  (not shown). Note that these two models are also favored by several other observations based on the 2dFGRS, such as the redshift-space clustering of galaxies (Yang et al. 2004a) and the multiplicity function of galaxy groups (Yang et al. 2004b).

Before concluding that therefore the satellite occupation statistics hint towards either a high  $(M/L)_{\text{cl}}$  or a low  $\sigma_8$ , it is important to check whether the  $L_{18}$  to  $M$  conversion (via the mean separation  $d$ ) used, has not introduced

any artifact in this statistic. To test this we determine the distribution of  $N_s$  directly from the populated haloes in the simulation box (i.e., without making a mock redshift surveys from which we select groups). Since we know the halo mass exactly for each halo in the box, we can compute the number of satellite galaxies above the magnitude limit listed. The resulting distributions of  $N_s$  are shown in Fig. 7 as thin solid lines and are in reasonable agreement with the distributions obtained from the corresponding MGRS (dotted lines). Although small differences are apparent, the overall trends, especially the dramatic overprediction of the mean satellite number, is nicely reproduced. This demonstrates that the discrepancy between 2dFGRS and MGRS is real, indicating that either cluster mass-to-light ratios are high or that  $\sigma_8 \sim 0.7$ .

### 3.3 Dependence on galaxy type

Madgwick et al. (2002) used a principal component analysis of galaxy spectra taken from the 2dFGRS to obtain a *spectral* classification scheme. They introduced the parameter  $\eta$ , a linear combination of the two most significant principal components, as a galaxy type classification measure. As shown by Madgwick et al. (2002),  $\eta$  follows a bimodal distribution and can be interpreted as a measure for the current star formation rate in each galaxy. Furthermore  $\eta$  is well correlated with *morphological* type (Madgwick 2002). In what follows we adopt the classification suggested by Madgwick et al. and classify galaxies with  $\eta < -1.4$  as ‘early-types’ and galaxies with  $\eta \geq -1.4$  as ‘late-types’. Each galaxy in our MGRS is assigned a type (early or late), using the method described in Yang et al. (2004a).

As shown in van den Bosch et al. (2003a), the observed correlation lengths of early and late type galaxies in the 2dFGRS indicate that the former are preferentially hosted by massive haloes. However, these data alone do not contain sufficient information to accurately constrain the segregation of the galaxy population in early and late types. Here we use the galaxy groups selected from the 2dFGRS to directly constrain the occupation statistics of both populations. Fig. 8 plots the fraction of early-type galaxies as a function of halo mass. Results are shown separately for all (central plus satellite) galaxies (left-hand panel) and for central galaxies only (right-hand panel). The solid, dotted and dashed lines correspond to the ‘mass-limited’ group samples V2, V3 and V4, respectively (see Table 1). Among the total population, the fraction of early-type galaxies increases from about 25% in haloes with  $M \sim 10^{12} h^{-1} M_\odot$  to about 80% in haloes with  $M \sim 10^{15} h^{-1} M_\odot$ . Among the central galaxy population, the increase of the fraction of early types with mass is stronger: in haloes with  $M \gtrsim 10^{14} h^{-1} M_\odot$  virtually all central galaxies are early types. As a comparison, the open circles with errorbars in Fig. 8 show the results obtained from the ‘mass-limited’ group samples (V2 in Table 1) constructed from the fiducial MGRSs. The model predictions agree reasonably well with the observational results, indicating that our model for splitting galaxies in early- and late-types (see van den Bosch et al. 2003a) is sufficiently accurate.

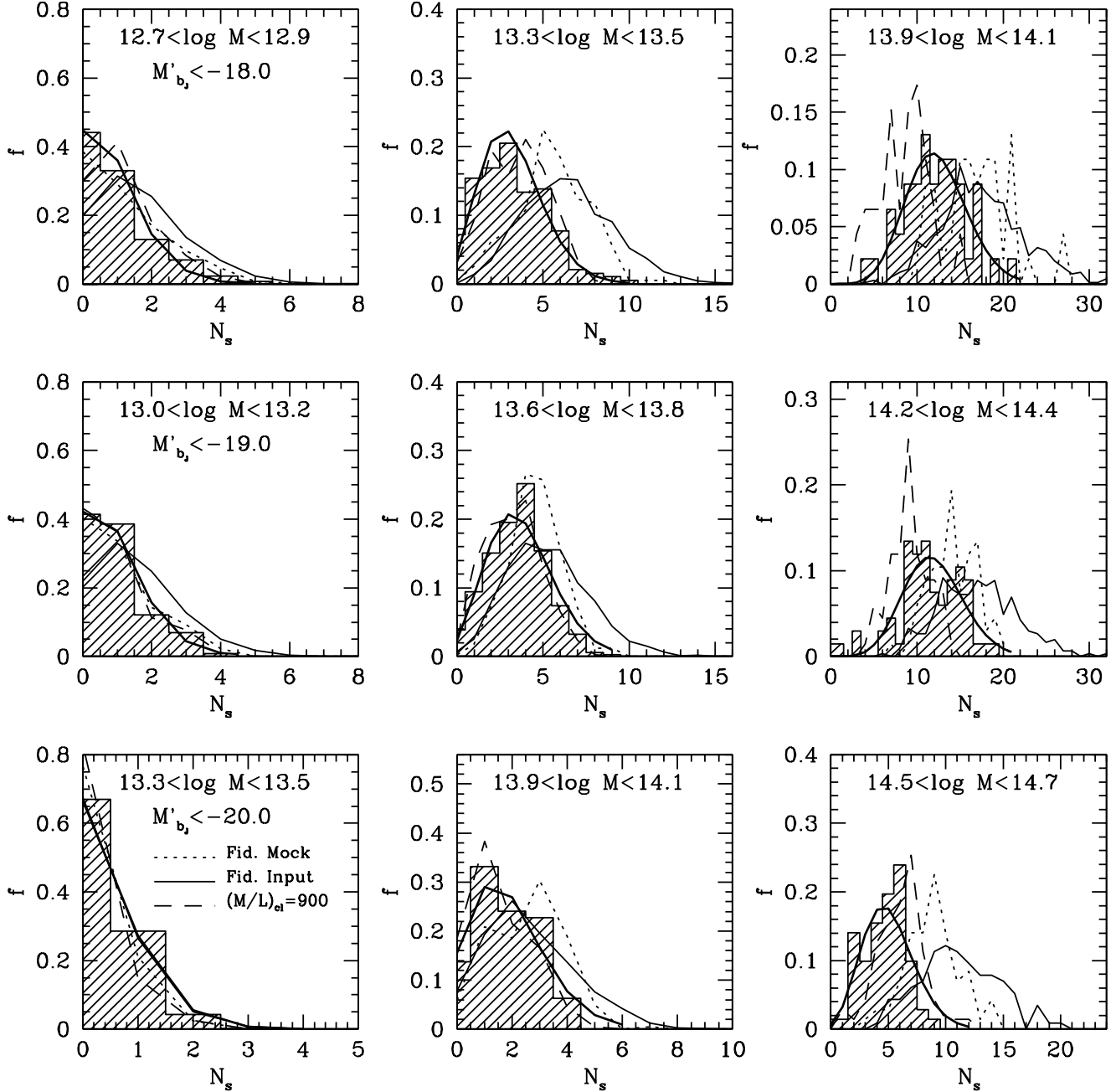


**Figure 7.** Distributions of the number of satellite galaxies in groups for different bins in halo mass, as indicated. Panels in the upper, middle and lower rows correspond to different absolute magnitude limits as indicated, where  $M'_{b_J} = M_{b_J} - 5 \log h$ . The hatched histograms indicate the distributions obtained from the groups in the 2dFGRS. Thick solid curves correspond to Poisson distributions with the same mean  $N_s$ , and are shown to illustrate the Poissonian nature of  $P(N_s|M)$ . The dotted and dashed histograms indicate the distributions obtained from the fiducial MGRS and the MGRS with  $(M/L)_{cl} = 900h (M/L)_\odot$ , respectively. Whereas the former dramatically overestimates the average number of satellite galaxies in massive haloes, the latter fits the 2dFGRS results extremely well. The thin, solid lines, are the number distributions of satellite galaxies obtained directly from the populated haloes in our fiducial simulation box (i.e., without making a mock redshift surveys from which we select groups). These therefore reflect the true  $P(N_s|M)$ . Note the good, overall agreement with the distributions obtained from the fiducial MGRS (dotted curves).

#### 4 THE CONDITIONAL LUMINOSITY FUNCTION

ditional luminosity function,  $\Phi(L|M)$ , which specifies the number of galaxies in haloes *as a function of luminosity*.

Thus far our discussion has only focused on the occupation *number* of galaxy groups (dark matter haloes). We now use the groups in the 2dFGRS to directly determine the con-

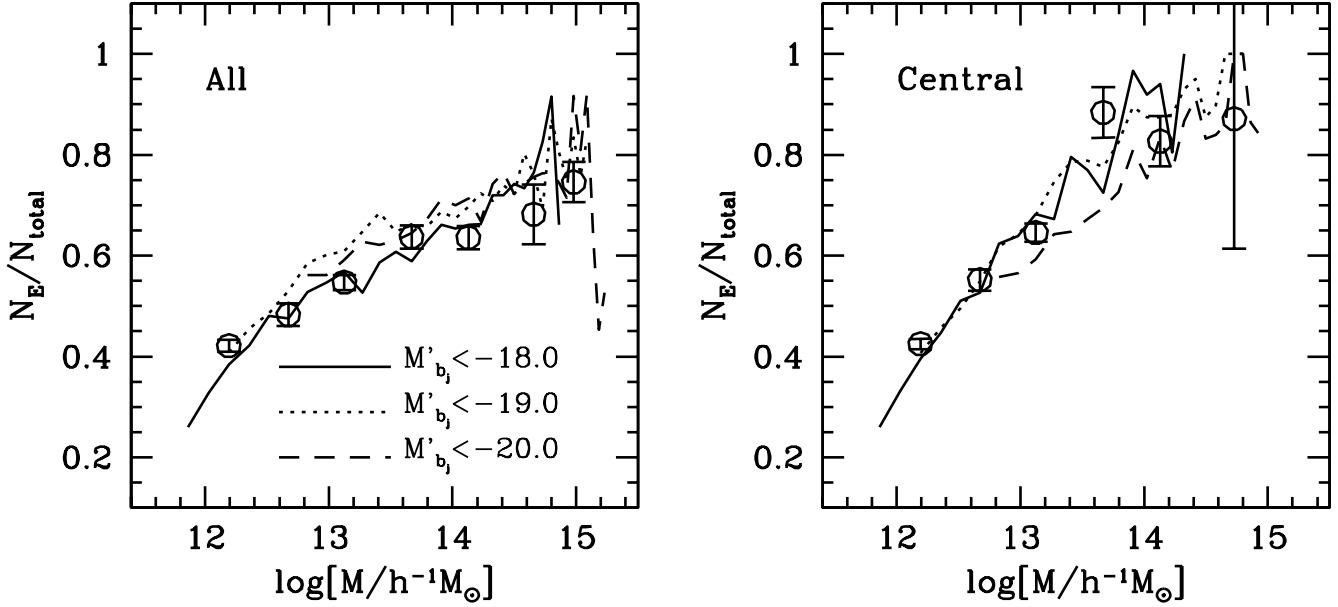


**Figure 8.** *Left-hand panel:* The fraction of early-type galaxies in groups of the 2dFGRS as function of halo mass. Solid, dotted and dashed lines correspond to the ‘mass-limited’ group samples V2, V3, and V4 with different absolute magnitude limits, respectively (see Table 1). As a comparison, the results for groups in the fiducial MGRSs with  $M_{b_J} - 5 \log h < -18.0$  are shown as circles with errorbars ( $1\text{-}\sigma$  scatter among 8 fiducial MGRSs). *Right-hand panel:* Same as left-hand panel, except that now only central galaxies are considered.

#### 4.1 Direct measurement of the CLF from 2dFGRS groups

The left-hand panels of Fig. 9 show the conditional luminosity functions (CLFs) of galaxies for 2dFGRS groups of different masses. For comparison, the contributions from satellite galaxies are shown separately. These CLFs have been obtained directly by counting galaxies in groups. For a given galaxy luminosity  $L$ , there is a limiting redshift,  $z_L$ , beyond which galaxies with such a luminosity are not included in the sample. In order to estimate the CLF,  $\Phi(L|M)$ , at given  $L$  and  $M$  we only use groups with mass  $M$  that are within the redshift limit  $z_L$ . The errorbars shown correspond to  $1\text{-}\sigma$  fluctuations among 8 independent MGRSs and reflect the expected errors due to cosmic variance. To test the reliability of the measurements, we compare in the middle panels the model input CLFs (solid curves) with those obtained from the mock group samples. The CLFs recovered from the groups in the MGRS agree well with the model input down to halo masses of  $M \sim 10^{13.3} h^{-1} M_\odot$ . For less massive haloes, however, there is a significant discrepancy. In particular, the CLFs determined from the groups seem to predict too few faint satellite galaxies, and too many bright central galaxies. There are two potential sources for these discrepancies: (i) the inaccuracy of our group finder for poor systems; (ii) the error in the  $L_{18}$  to  $M$  conversion. In order to test these possibilities, the right-hand panels of Fig. 9 plot the CLFs for MGRS groups binned according to true halo mass instead of the  $L_{18}$  ranking. This solves the problem at the bright end, suggesting that this particular discrepancy owes to errors in the  $L_{18}$ - $M$  conversion, but still results in too few faint galaxies. This reflects the incompleteness of our group finder (see Yang et al. 2004b). Note that, in low-mass haloes where  $L_{18}$  is dominated by the central galaxy, the  $L_{18}$ - $M$  conversion produces an artificial peak in the CLF

at the bright end (see the bottom middle panel). Such a peak is also seen in the observational data (the bottom left panel), but our tests show that it is doubtful that this is a real feature of the CLF.

These results are interesting in light of the recent findings by Zheng et al. (2004), who computed the conditional baryonic mass functions (hereafter CMF) of galaxies in the semi-analytical models of Cole et al. (2000). In haloes with  $12.5 \lesssim \log[M/M_\odot] \lesssim 14.0$  these CMFs reveal a clear peak due to the central galaxies. Before we can claim that this is inconsistent with our results presented above, we need to show that if a peak is present in the CLF, our analysis is able to recover it. To test this, we construct eight MGRSs based on CLFs that contain artificial peaks at the bright end, similar to the CMFs in Zheng et al. (2004). The input CLFs are shown as the solid curves in Fig. 10. We then apply all the observational selections to these MGRSs and select groups using exactly the same method as that for the real groups. The recovered CLFs in different mass ranges are shown in Fig. 10 as the histograms (the errorbars are  $1\text{-}\sigma$  scatter among the eight MGRSs). Comparing these with the model input, we see that our analysis is able to recover prominent peaks in the CLFs, although weak and sharp features may be smeared out. Thus, if the CLF for haloes with  $M \lesssim 10^{13.5} h^{-1} M_\odot$  indeed contained peaks as prominent as those predicted by the semi-analytical model mentioned above, our analysis would have easily revealed them. Therefore we conclude that the true CLF, as extracted from the 2dFGRS, does not reveal any prominent peaks. This suggests a problem for the semi-analytical models of Cole et al. (2000), although we caution that any disagreement between the CLF (based on luminosity in the photometric  $b_J$ -band) and the CMF (based on baryonic mass) should be interpreted with extreme care.

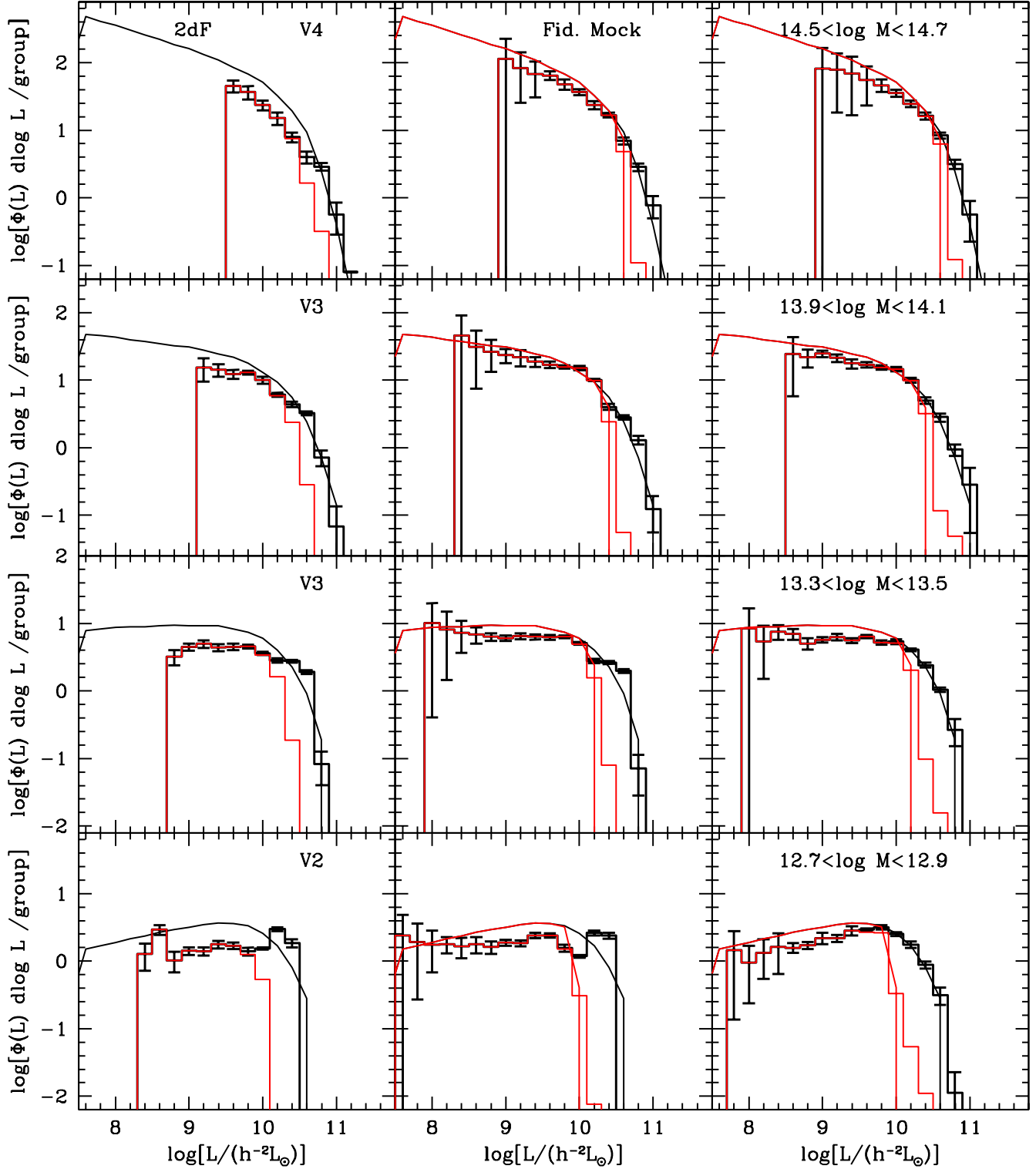


**Figure 9.** The conditional luminosity functions for groups in different mass bins, as indicated. Results are shown separately for all (central plus satellite) galaxies (the broader histogram) and satellite galaxies (the narrower histogram), respectively. The left-hand panels are for 2dF groups, while the middle panels are for groups in the fiducial MGRSs. In all these cases, halo masses are based on the rank-ordering of the group  $L_{18}$  luminosities. To test the impact of the error in the  $L_{18}$ - $M$  conversion, we show in the right panels the CLFs obtained from the fiducial MGRSs with groups binned according to their *true* halo masses. Errorbars in all panels are obtained from the  $1\text{-}\sigma$  scatter among the 8 fiducial MGRSs. As a comparison, the solid curves indicate the input CLFs (which are of Schechter form) used to construct the fiducial MGRSs.

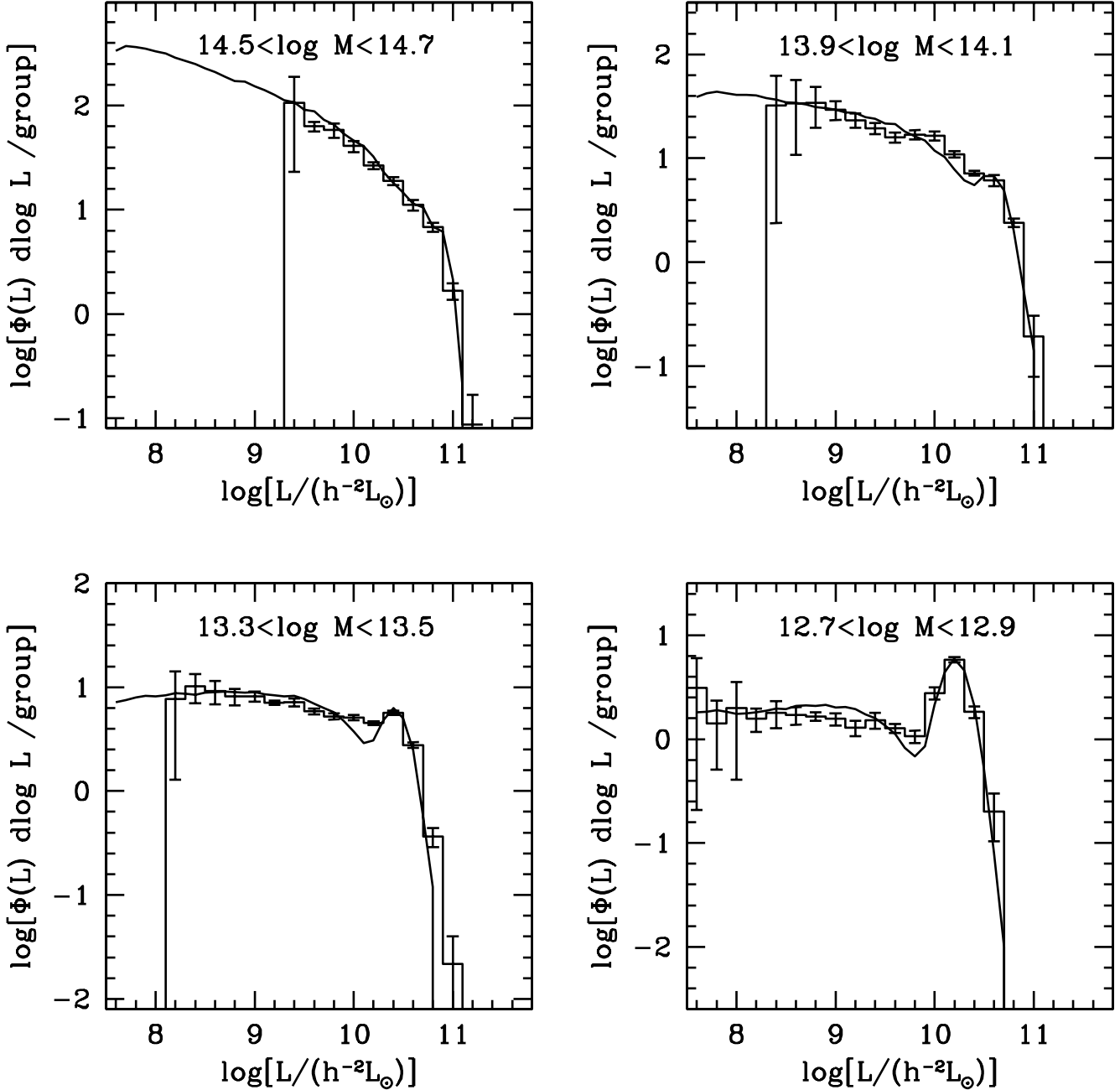


**Figure 10.** The conditional luminosity functions for groups in different mass bins, as indicated. The solid curves show the input CLFs, which contain peaks at the bright end to mimic the conditional baryonic mass functions found by Zheng et al. (2004). The histograms are the CLFs recovered from the groups selected from the MGRSs constructed with these input CLFs. Errorbars in all panels are based on the  $1\text{-}\sigma$  scatter among 8 MGRSs.

#### 4.2 Comparison with CLF Models

Having measured the CLFs from the groups in the 2dFGRS, we now turn to a comparison with the results obtained from the MGRSs and with the actual input CLFs used to construct them. Recall that the input CLFs are based on matching the observed luminosity function of galaxies and the luminosity-dependence of the correlation length of galaxies. Comparing the 2dF results shown in the left-hand panels of Fig. 9 with the results obtained from the fiducial MGRSs (the middle panels), we see that the observed CLFs

have shapes that are similar to our model predictions, but with a lower amplitudes. This is simply another reflection of the discrepancy between the 2dFGRS and our fiducial CLF model regarding the abundances of satellite galaxies (see Section 3.2 and also van den Bosch et al. 2004b). Similar discrepancies have previously been noticed from the pairwise peculiar velocity dispersions (Yang et al. 2004a) and the multiplicity function of galaxy groups (Yang et al. 2004b). As shown in these studies, these discrepancies indicate either a relatively high mass-to-light ratio on cluster scales, or a relatively low value of  $\sigma_8$ . To test how the corresponding CLF

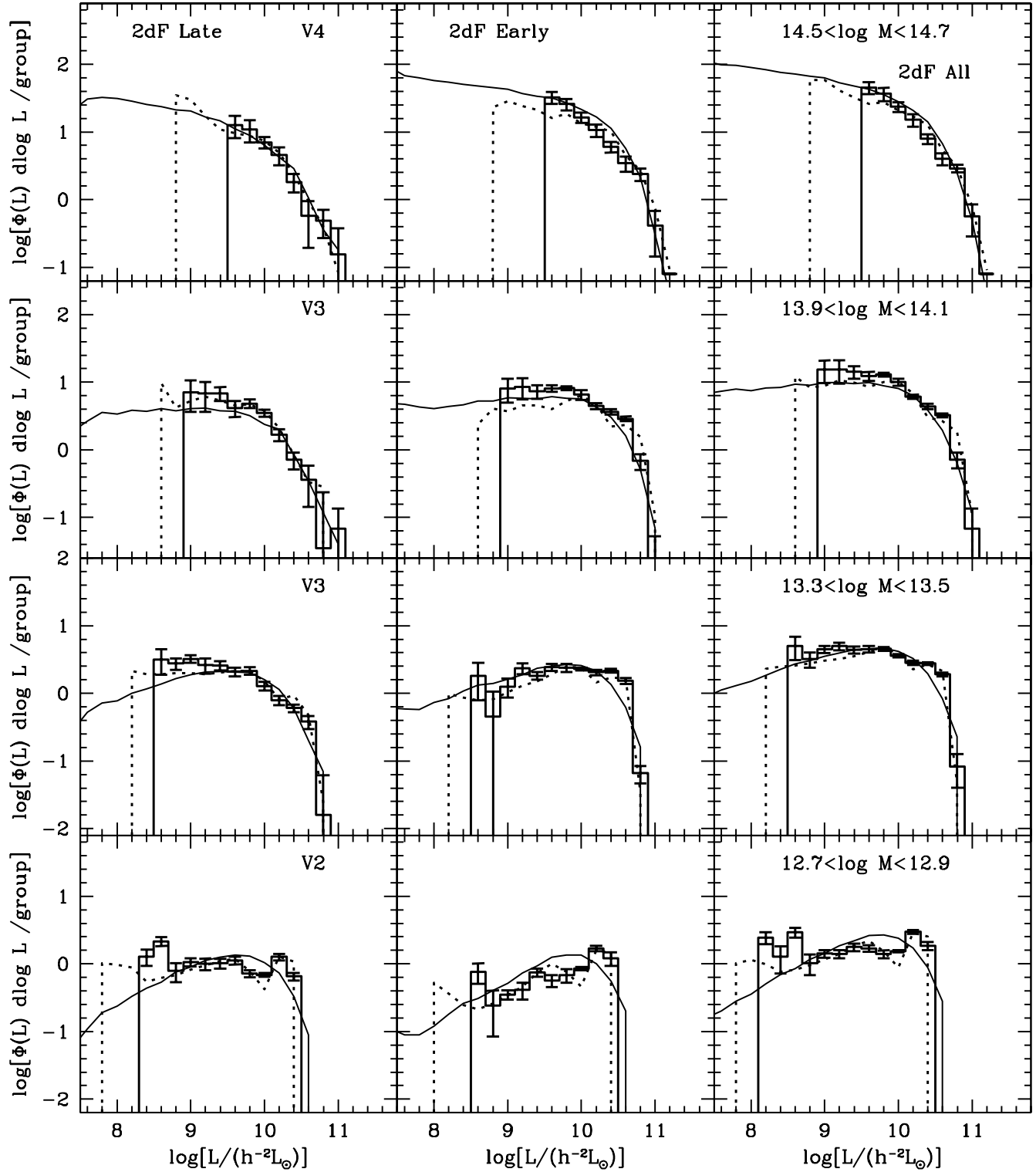


**Figure 11.** The conditional luminosity functions for 2dF groups in different mass bins (histograms), as indicated. Results are shown separately for late-type galaxies (left panels), early-type galaxies (middle panels) and all (early- and late-type) galaxies (right panels). Errorbars in all panels are obtained from the  $1\text{-}\sigma$  scatter among 8 MGRSs. The solid curves indicate the input CLFs used to construct the MGRSs with  $(M/L)_{cl} = 900h$ . The dotted lines are the CLFs recovered from the groups in these MGRSs, with halo masses estimated from the  $L_{18}$  ranking.

models compare to the CLF derived directly from the groups in the 2dFGRS, the dotted lines in Fig. 11 indicate the CLFs obtained from the MGRSs with  $(M/L)_{\text{cl}} \simeq 900h (M/L)_{\odot}$ . Results are shown separately for early-type, late-type, and all galaxies. Clearly, this model is in much better agreement with the 2dFGRS than the fiducial model. Note that the model also very nicely reproduces the CLFs of the early- and late-type galaxies separately. As for our fiducial mocks, the input CLFs (solid smooth curves) are well reproduced by the MGRSs for haloes more massive than  $10^{13.3} h^{-1} M_{\odot}$ , while for less massive haloes a small peak arises and the groups become incomplete at the faint end.

Unfortunately, we do not have a set of numerical simulations for a  $\Lambda$ CDM cosmology with  $\sigma_8 = 0.7$ , so that we can not construct corresponding MGRSs (but see Yang et al. 2004a for an approximate method). However, numerous tests discussed in our previous work suggests that this model is virtually indistinguishable from that with  $\sigma_8 = 0.9$  and  $(M/L)_{\text{cl}} \simeq 900h (M/L)_{\odot}$ . We therefore conclude that the CLFs determined directly from the groups in 2dFGRS provide further support for both models as viable descriptions of the galaxy-dark matter connection.

## 5 CONCLUSIONS

Using the galaxy group catalogue constructed from the 2dFGRS by Yang et al. (2004b), we have investigated various aspects regarding the halo occupation statistics of galaxies in the 2dFGRS. This is the first time the halo occupation distribution in real galaxy systems is examined in such detail, and has resulted in a number of interesting results that shed light on the connection between galaxies and dark matter haloes.

In order to estimate halo masses associated with the galaxy groups, we have ranked groups according to their group luminosity. Under the ansatz that the group luminosity is tightly correlated with halo mass, this is similar to mass ranking, and one can use the mean separation between the groups above a given ranking to determine the corresponding halo mass. Since any stochasticity in the relation between group luminosity and halo mass causes errors in the derived group masses, it is essential to use mock galaxy redshift surveys (MGRSs) to properly interpret the results. In this study we used MGRSs constructed using the conditional luminosity function (CLF) which has been constrained by the abundance and clustering properties of the galaxies in the 2dFGRS.

The first statistic we have investigated is the mean occupation number of galaxies above a given luminosity limit. Using the MGRS we have shown that this statistic can be determined from the galaxy groups extremely reliably, except for low mass haloes where  $\langle N \rangle \simeq 1$ . Here the stochasticity in the occupation statistics causes a systematic error that mimics a flat shoulder and a sharp break in the derived  $\langle N \rangle_M$ . Yet, the comparison between 2dFGRS and MGRS, both of which suffer from the same systematic, is meaningful and allows one to test whether the occupation statistics used to construct the MGRS (i.e., the CLF and its sampling strategy) are in agreement with the data. In terms of the mean occupation numbers, we find that our fiducial MGRS overestimates  $\langle N \rangle$  in high mass

haloes with respect to the 2dFGRS. This overabundance of satellite galaxies in massive haloes was previously noticed in van den Bosch et al. (2004b) and Yang et al. (2004b), and indicates that either clusters have an average mass-to-light ratio of  $(M/L)_{\text{cl}} \simeq 900h (M/L)_{\odot}$  (compared to  $(M/L)_{\text{cl}} = 500h (M/L)_{\odot}$  in our fiducial model), or that the power-spectrum normalization is relatively low;  $\sigma_8 \simeq 0.7$  rather than 0.9. Similar conclusions were reached by Yang et al. (2004a) from a detailed analysis of the pairwise-peculiar velocity dispersions of galaxies in the 2dFGRS.

In addition to the mean, we have also investigated the scatter in the occupation statistics, using the ratio  $\sigma(N)/\sqrt{\langle N \rangle}$ . In massive haloes we find this ratio to be close to unity, indicating that the occupation distribution  $P(N|M)$  is close to Poissonian. In low mass, haloes, however, there is a pronounced minimum indicating a  $P(N|M)$  that is significantly narrower than a Poisson distribution. We have shown that these findings are in excellent agreement with our fiducial MGRSs, but only if we sample the luminosity of the brightest galaxy in each halo in a somewhat deterministic way. Without such special treatment, i.e., when drawing all luminosities at random from the CLF, the ratio  $\sigma(N)/\sqrt{\langle N \rangle}$  is no longer in agreement with that of the 2dFGRS. These findings suggest that (i) the occupation statistics of central galaxies are sub-Poissonian, indicating some deterministic behavior in galaxy formation, and (ii) the number of satellite galaxies above a certain luminosity limit follows a Poissonian distribution. This is in excellent agreement with a scenario in which satellite galaxies are associated with dark matter subhaloes, which, as shown by Kravtsov et al. (2004), also follow Poissonian occupation statistics.

The mean luminosity of the central galaxies,  $L_c$ , is found to scale with halo mass as  $L_c \propto M^{2/3}$  for haloes with masses  $M < 10^{13} h^{-1} M_{\odot}$ , and as  $L_c \propto M^{1/4}$  for more massive haloes. At the low-mass end, this is in excellent agreement with results based on galaxy-galaxy weak lensing, which imply that  $M \propto L_c^{1.5}$  (e.g. Yang et al. 2003a; Guzik & Seljak 2002). The characteristic break at  $M \simeq 10^{13} h^{-1} M_{\odot}$  indicates the existence of a characteristic scale in galaxy formation, thought to be associated with the transition from effective to ineffective cooling (e.g., White & Rees 1978; Dekel 2004). Although not directly revealed by our galaxy groups, another characteristic mass,  $M \simeq 10^{11} h^{-1} M_{\odot}$ , can be inferred from our CLFs obtained from the 2dFGRS. Below this mass, star formation efficiency decreases rapidly with decreasing halo mass, presumably due to feedback from supernovae. We have also investigated the full distribution of central luminosity;  $P(L_c|M)$ . Although it appears log-normal, detailed tests show that the group luminosity ranking used to estimate halo masses causes systematic errors in  $P(L_c|M)$  (though the mean is not affected). The comparison with the MGRS, however, is still meaningful and shows excellent agreement, providing further support for the CLF and its sampling strategy.

In addition to a split in central and satellite galaxies, we have also divided the population in early- and late-type galaxies. The central galaxies in low-mass haloes are found to be predominantly late type galaxies, while those in massive haloes are almost entirely early types. This is in good agreement with the occupation statistics obtained from an



analysis of the clustering properties of early- and late-type galaxies (van den Bosch et al. 2003a).

Using the 2dF groups, we have also measured the conditional luminosity function directly. Although the CLF of central galaxies is fairly narrow, the presence of central galaxies does not show up as a strong peak at the bright end of the total CLF. In fact, over the entire halo mass range that can be reliably probed with the present data (from  $\sim 10^{13.3} h^{-1} M_{\odot}$  to  $\sim 10^{14.7} h^{-1} M_{\odot}$ ), the CLF is well fit by a Schechter function. This supports the assumption regarding the shape of the CLF made in our previous work, but disagrees with the conditional baryonic mass function (CMF) in semi-analytical models of galaxy formation. As shown by Zheng et al. (2004), the latter reveals a pronounced peak due to the central galaxies. We caution, however, that any disagreement between the CLF (based on luminosity in the photometric  $b_J$ -band) and the CMF (based on baryonic mass) should be interpreted with care.

The CLFs obtained from the galaxy groups in the 2dFGRS are in good agreement with the CLF model based on matching the observed luminosity function and large-scale clustering properties of galaxies in the  $\Lambda$ CDM concordance cosmology. It indicates that this model provides an accurate description of the connection between galaxies and dark matter haloes, with the condition that either  $\sigma_8 \simeq 0.7$ , or, if  $\sigma_8 = 0.9$ , that clusters have a mass-to-light ratio that is significantly higher than typically found. Finally we point out that, with the completion of the SDSS, the analysis presented here can be naturally extended to include a wider variety of intrinsic properties of individual galaxies (in addition to luminosity and type), to investigate the occupation statistics as function of color, surface brightness, AGN activity, etc. The results from such analyses will provide unprecedented constraints on how galaxies of different physical properties form in dark matter haloes of different masses.

## ACKNOWLEDGEMENT

Numerical simulations used in this paper were carried out at the Astronomical Data Analysis Center (ADAC) of the National Astronomical Observatory, Japan. We thank the 2dF team for making their data publicly available and the anonymous referee for many valuable comments. FB thanks Peder Norberg for vivid discussions on groups in the 2dFGRS.

## REFERENCES

- Abazajian K., et al., 2004, preprint (astro-ph/0408003)  
Bahcall N.A., Cen R., Davé R., Ostriker J.P., Yu Q., 2000, ApJ, 541, 1  
Baugh C.M., The 2dFGRS team, 2004, MNRAS, 351, L44  
Benson A.J., Cole S., Frenk C.S., Baugh C.M., Lacey C.G., 2000, MNRAS, 311, 793  
Benson A.J., Bower R.G., Frenk C.S., Lacey C.G., Baugh C.M., Cole S., 2003, ApJ, 599, 38  
Berlind A.A., Weinberg D.H., 2002, ApJ, 575, 587  
Berlind A.A., Weinberg D.H., Benson A.J., Baugh C.M., Cole S., Dave R., Frenk C.S., Jenkins A., Katz N., Lacey C.G., 2003, ApJ, 593, 1  
Bullock J.S., Wechsler, R.H., Somerville R.S., 2002, MNRAS, 329, 246  
Carlberg R.G., Yee H.K.C., Ellingson E., Abraham R., Gravel P., Morris S., Pritchet C.J., 1996, ApJ, 462, 32  
Cole C., Lacey C.G., Baugh C.M., Frank C.S., 2000, MNRAS, 319, 168  
Colless M., et al., 2001, MNRAS, 328, 1039  
Dekel A., 2004, preprint (astro-ph/0401503)  
Dekel A., Silk J., 1986, ApJ, 303, 39  
Eke V.R., The 2dFGRS team, 2004, MNRAS, 348, 866  
Guzik J., Seljak U. 2002, MNRAS, 335, 311  
Jing Y.P., Börner G., Suto Y., 2002, ApJ, 564, 15  
Jing Y.P., Mo H.J., Börner G., 1998, ApJ, 494, 1  
Kang X., Jing Y.P., Mo H.J., Börner G., 2002, MNRAS, 336, 892  
Kang X., Jing Y.P., Mo H.J., Börner G., 2004, submitted to ApJ, preprint (astro-ph/0408475)  
Kauffmann G., White S.D.M., Guiderdoni B., 1993, MNRAS, 264, 201  
Kepner J., Fan X., Bahcall N., Gunn J., Lupton R., Xu G., 1999, ApJ, 517, 78 preprint (astro-ph/0401578)  
Kim R.J.S., et al. 2002, AJ, 123, 20  
Kravtsov A.V., Berlind A.A., Wechsler R.H., Klypin A.A., Gottlöber S., Allgood B., Primack J.R., 2004, ApJ, 609, 35  
Kochanek C.S., White M., Huchra J., Macri L., Jarrett T.H., Schneider S.E., Mader J., 2003, ApJ, 585, 161  
Lin Y.T., Mohr J.J., 2004, preprint (astro-ph/0408557)  
Madgwick D.S., et al. , 2002, MNRAS, 333, 133  
Magliocchetti M., Porciani C., 2003, MNRAS, 346, 186  
Marinoni C., Hudson M.J., 2002, ApJ, 569, 101  
Mo H.J., Yang X.H., van den Bosch F.C., Jing Y.P., 2004, MNRAS, 349, 205  
Norberg P., et al., 2002, MNRAS, 336, 907  
Peacock J.A., Smith R.E., 2000, MNRAS, 318, 1144  
Postman M., et al., 1996, AJ, 111, 615  
Rozo E., Dodelson S., Frieman J.A., 2004, PhRvD., 70, 3008  
Seljak U., 2000, MNRAS, 318, 203  
Scoccimarro R., Sheth R.K., Hui L., Jain B., 2001, ApJ, 546, 20  
Scranton R., 2002, MNRAS, 332, 697  
Tully R.B., 2003, ApJ, in press, preprint (astro-ph/0312441)  
Vale A., Ostriker J.P., 2004, MNRAS, 353, 189  
van den Bosch F.C., Yang X.H., Mo H.J., 2003a, MNRAS, 340, 771  
van den Bosch F.C., Mo H.J., Yang X.H., 2003b, MNRAS, 345, 923  
van den Bosch F.C., Norberg P., Mo H.J., Yang X.H., 2004a, MNRAS, 352, 1302  
van den Bosch F.C., Yang X.H., Mo H.J., Norberg P., 2004b, MNRAS, in press (astro-ph/0406246)  
Wang Y., Yang X.H., Mo H.J., van den Bosch F.C., Chu Y., 2004, MNRAS, 353, 287  
White S.D.M., Rees M.J., 1978, MNRAS, 183, 341  
White M., Kochanek C.S., 2002, ApJ, 574, 24  
Yan R., Madgwick D.S., White M., 2003, ApJ, 598, 848  
Yan R., White M., Coil A.L., 2004, ApJ, 607, 739  
Yang X.H., Mo H.J., Kauffmann Guinevere, Chu Y.Q., 2003a, MNRAS, 339, 387  
Yang X.H., Mo H.J., van den Bosch F.C., 2003b, MNRAS, 339, 1057  
Yang X.H., Mo H.J., Jing Y.P., van den Bosch F.C., Chu Y.Q., 2004a, MNRAS, 350, 1153  
Yang X.H., Mo H.J., van den Bosch F.C., Jing Y.P., 2004b, MNRAS, in press (astro-ph/0405234) (YMBJ)  
Yang X.H., Mo H.J., van den Bosch F.C., Jing Y.P., 2004c, MNRAS, in press (astro-ph/0406593)  
Zehavi I., et al., 2004a ApJ, 608, 16  
Zehavi I., et al., 2004b ApJ, preprint (astro-ph/0408569)  
Zheng Z., Tinker J.L., Weinberg D.H., Berlind A.A., 2002, ApJ, 575, 617  
Zheng Z., et al., 2004, ApJ, preprint (astro-ph/0408564)